Universität Stuttgart

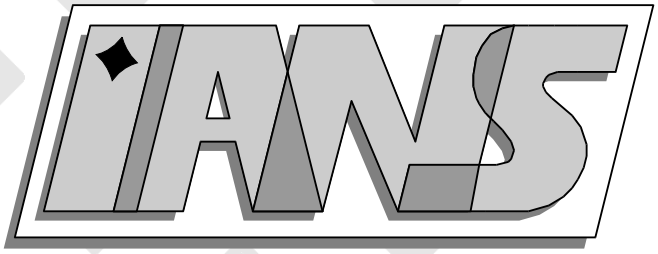

Multigrid methods for unresolved Dirichlet boundaries

Alexander Weiss, Barbara Wohlmuth

Berichte aus dem Institut für Angewandte Analysis und Numerische Simulation

Preprint 2005/011

Universität Stuttgart

Multigrid methods for unresolved Dirichlet boundaries

Alexander Weiss, Barbara Wohlmuth

Berichte aus dem Institut für Angewandte Analysis und Numerische Simulation

Preprint 2005/011

Institut für Angewandte Analysis und Numerische Simulation (IANS)
Fakultät Mathematik und Physik
Fachbereich Mathematik
Pfaffenwaldring 57
D-70 569 Stuttgart

E-Mail: ians-preprints@mathematik.uni-stuttgart.de
WWW: http://preprints.ians.uni-stuttgart.de

ISSN **1611-4176**

MULTIGRID METHODS FOR UNRESOLVED DIRICHLET BOUNDARIES

A.A. WEISS* AND B.I. WOHLMUTH*

Abstract. In this paper, multigrid methods are studied for elliptic boundary value problems where the change between Dirichlet and Neumann boundary conditions is not resolved by the sequence of triangulations. Starting from conforming P1 finite elements, three sequences of subspaces are considered and optimal multigrid convergence rates are shown for these approaches. The first class of spaces is defined by enlarging the Dirichlet boundary which results in a conforming approach. It is shown that these spaces still satisfy an approximation property. By reducing the Dirichlet boundary, one obtains non-conforming finite element spaces. The third class is obtained by a hierarchical modification of the finite element basis. This leads to conforming and nested finite element spaces. In numerical examples the performance of the proposed variants is illustrated for the Laplace and Lamé equation. Although for all approaches, the convergence rate is bounded independently of the mesh size, not all approaches result in satisfactory convergence rates.

Key words. optimal multigrid convergence rates, iterative solver, non-nested space, non-conforming elements

AMS subject classifications. 65N30, 65N55

1. Introduction. Multigrid methods [1, 6, 14] have shown to be a very fast and efficient iterative solvers for the finite-element discretization of elliptic boundary problems. In contrast to standard iterative solvers, with multigrid methods one obtains optimal convergence rates which are independent of the meshsize. Moreover, in many cases the proportionality constant is very small so that these methods provide powerful solvers for the elliptic systems.

In the last decades, these methods have evolved to handle complex systems appearing in engineering problems such as in structural mechanics, coupled systems and low-regularity problems. Therefore, it was neccecary to enhance the analysis to situations where the problem does not have H^2-regularity and to spaces that are non-conforming or not nested.

Multigrid convergence proofs for problems without full regularity have been given in, e.g. [9, 11]. Application to non-nested and non-conforming finite element spaces has also been developed, see, e.g., [7, 10, 18]. Recently, multigrid methods have been constructed for complex applications. These include multigrid methods for mortar couplings, [4, 5] and monotone multigrid algorithms to solve contact problems, e.g. [17, 21].

When considering contact problems, changes in the boundary conditions naturally occur. The variational inequality can be written as a free boundary value problem. Dirichlet boundary conditions have to be imposed on the displacements in the normal direction on the actual contact set which is a priori unknown. On the complementary part, homogeneous Neumann boundary conditions apply. When using multigrid methods, these changes in the boundary conditions are not necessarily resolved by the coarser grids.

In this paper, we present three approaches to deal with problems where the Dirichlet boundary is not resolved by the triangulation. For the conforming and nested approaches, we obtain optimal multigrid convergence for the V- and W-cycle algorithm. For the non-conforming approach, we obtain optimal convergence for the W-cycle algorithm.

We consider a second order boundary value problem,

$$\begin{aligned} Lu := -\operatorname{div}(A\nabla u) &= f \qquad \text{in } \Omega, \\ u &= 0 \qquad \text{on } \Gamma_D, \\ n_\Gamma^T A\nabla u &= g_N \qquad \text{on } \Gamma_N, \end{aligned} \tag{1.1}$$

in a polygonal, bounded domain $\Omega \subset \mathbb{R}^2$ with a symmetric, positive definite matrix A, outer normal n_Γ, a closed Dirichlet boundary $\Gamma_D \subseteq \partial\Omega$, $\operatorname{meas}(\Gamma_D) > 0$, and a Neumann boundary $\Gamma_N = \partial\Omega \backslash \Gamma_D$. The weak formulation of the above problem is to find $u \in H^1_{0,D}(\Omega) := \{v \in H^1(\Omega), v|_{\Gamma_D} = 0\}$ such

*Institute of Applied Analysis and Numerical Simulations (IANS), Universität Stuttgart, Pfaffenwaldring 57, 70529 Stuttgart, Germany. email: {weiss,wohlmuth}@ians.uni-stuttgart.de.
This work was supported in part by the Deutsche Forschungsgemeinschaft, SFB 404, B8

that

$$a(u,v) = F(v) \quad \forall v \in H^1_{0,D}(\Omega), \tag{1.2}$$

where

$$a(u,v) := \int_\Omega (\nabla u(x))^\intercal A(x) \nabla v(x) dx, \quad F(v) := \int_\Omega f(x)v(x)dx + \int_{\Gamma_N} g_N(x)v(x)dx.$$

For mixed boundary conditions, we do not, in general, have full H^2-regularity, but only $H^{1+\alpha}$-regularity for $0 < \alpha < 1/2$, see, e.g., [13].

In this paper, we will use the notation $a \lesssim b$ to mean $a \leq Cb$ with a constant C independent of the variables occurring in a and b and independent of the meshsize h_k; $a \approx b$ means $a \lesssim b$ and $b \lesssim a$.

The rest of the paper is organized as follows. In Section 2, we construct the discrete spaces for three approaches and examine some basic properties. In Section 3 we consider the question of optimal multigrid convergence. In Section 3.1, the approximation property is established, and in Section 3.2 the smoothing property is examined. Finally in Section 4, we give some numerical results.

2. Construction of the discrete spaces. Let $\mathcal{T}_0$ be a regular simplicial triangulation such that $\Omega = \bigcup_{T\in\mathcal{T}_0} T$. By uniform refinement, we obtain a hierarchy of nested triangulations $\mathcal{T}_k$. We denote by $\mathcal{P}_k$ the set of vertices, by $\mathcal{E}_k$ the set of the closed edges, $E = \bar{E}$, of the triangulation $\mathcal{T}_k$, by V_k the P1 finite element spaces associated with the vertices of the triangulation $\mathcal{T}_k$, and by $\{\varphi^k_p, p \in \mathcal{P}_k\}$ the standard nodal basis of V_k. We note that we do not require that Γ_D is a union of edges in $\mathcal{E}_0$.

Considering the triangulation, we require the following assumptions:

(A1) For each $T \in \mathcal{T}_0$ there is at most one change in the boundary conditions on ∂T.

(A2) For each $p \in \mathcal{P}_0$ with $p \in \Gamma_D$, there exists an edge $E^0_p \in \mathcal{E}_0$ such that $p \in E^0_p$ and $E^0_p \subset \Gamma_D$.

For a given triangulation $\mathcal{T}_k$, we define the set $\mathcal{P}^-_k := \{p \in \mathcal{P}_k, p \notin \Gamma_D\}$ and the finite element space

$$V^-_k := \{\varphi^k_p, p \in \mathcal{P}^-_k\}.$$

This space can be seen as a finite element space defined with respect to a reduced Dirichlet boundary,

$$V^-_k = \{v \in V_k, v|_{\Gamma^-_{D,k}} = 0\},$$

where $\Gamma^-_{D,k}$ is given by

$$\Gamma^-_{D,k} := \bigcup \{E \in \mathcal{E}_k, E \subseteq \Gamma_D\},$$

as depicted in Figure 2.1. Note that assumption (A2) ensures $\mathrm{meas}(\Gamma^-_{D,k}) > 0$.

However, if Γ_D is not resolved by the triangulations $\mathcal{T}_k$, the spaces V^-_k are not conforming and because $\Gamma^-_{D,k} \not\supseteq \Gamma^-_{D,k+1}$ in general, not even nested. Therefore, we introduce a second family of spaces by setting

$$V^+_k := V_k \cap H^1_{0,D}(\Omega).$$

We note that the finite elements in V^+_k do not only satisfy homogeneous Dirichlet boundary condition on Γ_D, but also on its enlargement with respect to the triangulation $\mathcal{T}_k$ which is defined by

$$\Gamma^+_{D,k} := \bigcup \{E \in \mathcal{E}_k, \mathrm{meas}(E \cap \Gamma_D) \neq 0\}.$$

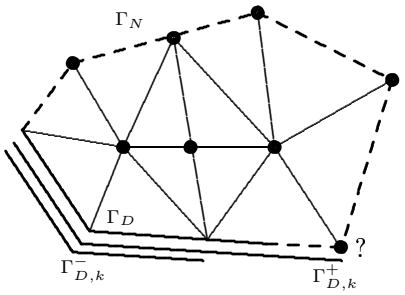

FIGURE 2.1. *Extended* $(\Gamma^+_{D,k})$ *and reduced* $(\Gamma^-_{D,k})$ *boundary sets.*

By definition, the spaces V_k^+ are conforming and because of $\Gamma^+_{D,k} \supseteq \Gamma^+_{D,k+1}$ also nested. Moreover, we find that $V_k^+ \subseteq V_k^-$. We note that if Γ_D is resolved by the triangulation $\mathcal{T}_k$, the two families of spaces $\{V_l^+, l \geq k\}$ and $\{V_l^-, l \geq k\}$ coincide.

Thus, by enlarging the Dirichlet-boundary on every level, we get conforming spaces which turn out to be automatically nested. Another approach to get nested spaces is by modifying the spaces V_k^-. Let $\pi^k : C(\bar{\Omega}) \to V_k^-$ be the Lagrange interpolation onto the space V_k^-,

$$\pi^k \xi := \sum_{p \in \mathcal{P}_k^-} \xi(p) \varphi_p^k.$$

For a fixed fine level K, we define the modification to be applied on the space V_k^- as a multiplicative application of the Lagrange interpolation operator,

$$\pi_k^K := \pi^K \circ \pi^{K-1} \circ \ldots \circ \pi^{k+2} \circ \pi^{k+1}, \quad \pi_K^K := Id.$$

The third family of finite element spaces is then defined by

$$\pi_k^K V_k^- := \{\pi_k^K v, v \in V_k^-\}, \quad k = 0, \ldots, K.$$

By this definition, we find that the elements in $\pi_k^K V_k^-$ are, in general, not finite elements associated with the mesh on level k. As a consequence, we cannot apply the inverse estimate to get a bound of the largest eigenvalue. We note that the spaces $\pi_k^K V_k^-$ have by definition the same dimension as the spaces V_k^-.

LEMMA 2.1. *The finite element spaces* $\pi_k^K V_k^-$ *are nested, i.e,* $\pi_k^K V_k^- \subseteq \pi_{k+1}^K V_{k+1}^-$.

Proof. For $w \in \pi_k^K V_k^-$, $0 \leq k < K$, there exists a $v \in V_k^-$ such that

$$w = \pi_k^K v = \pi_{k+1}^K \pi^{k+1} v.$$

As $\pi^{k+1} v \in V_{k+1}^-$ by definition, we obtain $w \in \pi_{k+1}^K V_{k+1}^-$. □

Because V_K^- is a non-conforming finite element space if the Dirichlet-boundary is not resolved by the triangulation $\mathcal{T}_K$, the spaces π_k^K, in general, turn out to be non-conforming finite element spaces. We use these spaces only as auxiliary spaces in the analysis of the smoothing property later.

Using a slightly different definition, we get conforming and nested spaces which is the third approach of this paper. At first we define the spaces which will be modified in the same way as before. Using the fixed fine level K, we denote by $\tilde{\Gamma}_D$ the Dirichlet boundary enlarged according to the grid on level K, $\tilde{\Gamma}_D := \Gamma^+_{D,K} \supseteq \Gamma_D$, and define the spaces $\tilde{V}_k^-$ as the non-conforming spaces with respect to the Dirichlet boundary $\tilde{\Gamma}_D$,

$$\tilde{V}_k^- := \{\varphi_p^k, p \in \tilde{\mathcal{P}}_k^-\}, \quad \text{where} \quad \tilde{\mathcal{P}}_k^- := \{p \in \mathcal{P}_k, p \notin \tilde{\Gamma}_D\}.$$

LEMMA 2.2. *For* $0 \leq k \leq K$, *the relation* $V_k^+ \subseteq \tilde{V}_k^- \subseteq V_k^-$ *holds.*

Proof. Using the definition of $\Gamma^+_{D,k}$ and $\tilde{\Gamma}_D$, we get

$$\Gamma^+_{D,k} \supseteq \Gamma^+_{D,K} = \tilde{\Gamma}_D \supseteq \tilde{\Gamma}^-_{D,k}.$$

On the other hand, we have $\tilde{\Gamma}_D \supseteq \Gamma_D$ and hence $\tilde{\Gamma}^-_{D,k} \supseteq \Gamma^-_{D,k}$. ☐ The spaces $\tilde{V}^-_k$ are now modified in the same way as before resulting in nested and conforming finite element spaces. We set

$$\tilde{\pi}^k : C(\bar{\Omega}) \to \tilde{V}^-_k, \quad \tilde{\pi}^k \xi := \sum_{p \in \tilde{\mathcal{P}}^-_k} \xi(p) \varphi^k_p,$$
$$\tilde{\pi}^K_k := \tilde{\pi}^K \circ \tilde{\pi}^{K-1} \circ \ldots \circ \tilde{\pi}^{k+2} \circ \tilde{\pi}^{k+1}, \quad \tilde{\pi}^K_K := Id.$$

The finite element spaces of our third approach are defined by

$$V^{\mathrm{mod}}_k := \tilde{\pi}^K_k \tilde{V}^-_k = \{\tilde{\pi}^K_k \tilde{v} : \tilde{v} \in \tilde{V}^-_k\}, \quad k = 0, \ldots, K.$$

LEMMA 2.3. *The finite element spaces V^{mod}_k are conforming and nested spaces satisfying $V^{mod}_K = V^+_K$. Furthermore, $V^+_k \subseteq V^{mod}_k$ for $0 \le k \le K$.*

Proof. That $V^{\mathrm{mod}}_k \subseteq V^{\mathrm{mod}}_{k+1}$ follows by the arguments used in Lemma 2.1. In addition, by definition $V^{\mathrm{mod}}_K = \tilde{V}^-_K$ and as $\tilde{\Gamma}_D = \Gamma^+_{D,K}$ is resolved on the finest grid, we get $\tilde{\Gamma}^-_{D,K} = \Gamma^+_{D,K}$ and therefore $V^{\mathrm{mod}}_K = V^+_K \subset H^1_{0,D}$.

Using Lemma 2.2, we obtain $V^+_k \subseteq V^+_l \subseteq \tilde{V}^-_l$ for $0 \le k \le l \le K$. Hence, $\tilde{\pi}^K_k|_{V^+_k} = \mathrm{Id}$ and furthermore $V^+_k = \tilde{\pi}^K_k V^+_k \subseteq \tilde{\pi}^K_k \tilde{V}^-_k = V^{\mathrm{mod}}_k$. ☐ As before, the elements in V^{mod}_k are not finite elements associated with the mesh on level k and therefore the standard inverse estimate cannot be used to get an appropriate bound of the largest eigenvalue.

We define the nodal basis function of V^{mod}_k by $\varphi^{\mathrm{mod},k}_p := \tilde{\pi}^K_k \varphi^k_p$, $p \in \tilde{\mathcal{P}}^-_k$. The operator $\tilde{\pi}^K_k$ applied to φ^k_p guarantees that $\varphi^{\mathrm{mod},k}_p \subset H^1_{0,D}(\Omega)$. This modification is carried out in a multiplicative way. We note that the dimension of the spaces V^{mod}_k coincide with the dimension of the spaces $\tilde{V}^-_k$ which is, in general, not equal to the dimension of the spaces V^-_k. However, if $\Gamma^-_{D,k} = \tilde{\Gamma}^-_{D,k}$, the dimensions are equal.

REMARK 2.4. *As we will see later, this hierarchical modification preserves the order of the largest eigenvalue of the stiffness matrix on each level k. This is not the case if we use the definition $\tilde{\pi}^K \tilde{V}^-_k$ for V^{mod}_k. In that situation, $\tilde{\pi}^K$ acts as a cut-off operator on $\tilde{V}^-_k$ with respect to the finest level and the largest eigenvalue is no longer bounded in terms of Ch^{-2}_k. Moreover, in that case, we do not obtain nested finite element spaces.*

3. Multigrid methods. The choice of V^+_k or V^{mod}_k leads to conforming and nested finite element spaces. For those spaces, there are two basic ingredients in a proof of optimal multigrid convergence rates for both W- and V-cycle algorithms, namely the approximation and the smoothing property, see, e.g., [3, 12, 14]

First, we define a discrete scalar product, $(\cdot,\cdot)_k$ by $(u,v)_k := h^2_k \sum_{p \in \mathcal{P}_k} u(p)v(p)$ and the operator $A_k : W_k \to W_k$ by $(A_k u, v)_k = a(u,v) \quad \forall u, v \in W_k$ for $W_k \in \{V^+_k, V^{\mathrm{mod}}_k\}$. The approximation and smoothing properties are given in terms of a scale of discrete energy norms defined by

$$\|\!| v |\!|^2_{s,k} := (A^s_k v, v)_k, \quad s \ge 0.$$

We note that with this definition, we have $\|\!| v |\!|_{0,k} \approx \|v\|_0$ and $\|\!| v |\!|^2_{1,k} = a(v,v) \approx \|v\|^2_1$. Using these discrete norms, the approximation property can be stated as

$$\|\!| (Id - P_{k-1}) v |\!|_{1,k} \lesssim h^s_k \, \|\!| v |\!|_{1+s,k}, \quad 0 \le s \le \alpha, \tag{3.1}$$

([12, p. 162] in the case of full elliptic regularity) and the smoothing property as

$$\|\!| R^m_k v |\!|_{1+s,k} \lesssim h^{-s}_k m^{s/2} \, \|\!| v |\!|_{1,k}, \quad 0 \le s \le \alpha, \tag{3.2}$$

([12, p. 164] in the case of full regularity) where P_{k-1} is the Galerkin-projection on the finite element space on level $k-1$ and R_k is the error propagation of the smoothing operator.

Let us first focus on the approximation property. Using Céa's lemma, we get

$$\|\!|(\mathrm{Id} - P_k)v|\!\|_{1,k} \approx \|(\mathrm{Id} - P_k)v\|_1 \lesssim \inf_{w \in W_k} \|v - w\|_1 .$$

As $s \leq \alpha < 1/2$, we know that $W_k \subset H^{1+s}(\Omega)$. We use the equivalence of norms proved in [11, Lemma 4.2], $\|\!|v|\!\|_{1+s,k} \approx \|v\|_{1+s}$ for $v \in W_k$, which hold if the approximation condition

$$\inf_{v \in W_k} \|\zeta - v\|_1 \lesssim h_k^s \|\zeta\|_{1+s} \quad \forall \zeta \in H^{1+s}_{0,D}(\Omega), \quad W_k \in \{V_k^+, V_k^{\mathrm{mod}}\}, \tag{3.3}$$

is fulfilled and the problem has $H^{1+\alpha}$-regularity. Here, $H^{1+s}_{0,D}(\Omega)$ is defined by $H^{1+s}_{0,D}(\Omega) := H^{1+s}(\Omega) \cap H^1_{0,D}(\Omega)$. Hence, it is sufficient to show that (3.3) holds.

For the smoothing property it is essential to estimate the largest eigenvalue of A_k. For example, using the Richardson relaxation as a smoothing operator, the smoothing property (3.2) follows directly from $\lambda_{\max}(A_k) \lesssim h_k^{-2}$, see, e.g., [1, 12, 14]. By the definition of the discrete norms, $\lambda_{\max}$ can easily be bounded by estimating $\|\!|v|\!\|^2_{1,k} \,/\, \|\!|v|\!\|^2_{0,k}$. Assuming that the inverse estimate holds, we conclude $\lambda_{\max}(A_k) \lesssim h_k^{-2}$.

For non-conforming and non-nested finite element spaces, the situation is more complex. However, comparing with a conforming and nested family of finite element spaces, it is possible to show optimal convergence of the W-cycle algorithm. The details of the W-cycle proof for non-conforming and non-nested spaces can be found, e.g., in [8, 10, 14].

We summarize what we have to do to show optimal multigrid convergence for our three approaches defined in Section 2.

- The spaces V_k^- are non-conforming and non-nested. We use the abstract framework in [10] and refer to [20], where the assumptions therein are proved for the spaces V_k^-. More precisely, conforming and nested spaces are defined using Lagrange interpolation operators similar to π^k such that the basis functions can be bijectively mapped to the basis of V_k^-. Furthermore, the stability of the bijection and the prolongation and the approximation properties are shown.
- The conforming and nested spaces V_k^+ are the smallest of our finite element spaces. The smoothing property is trivial since the inverse estimates holds, but we have to show the approximation property. In Section 3.1, we use a Scott–Zhang type interpolation operator and show that the approximation property still holds for unresolved boundary conditions.
- The spaces V_k^{mod} are also conforming and nested finite element spaces. The approximation property follow directly from $V_k^+ \subseteq V_k^{\mathrm{mod}}$, but the smoothing property is not obvious. As already pointed out, the elements in V_k^{mod} are not associated with the mesh on level k, but with the finest mesh. In Section 3.2, we show that the inverse estimate also holds for V_k^{mod} under some weak additional assumptions.

3.1. Approximation property. We use the following Scott–Zhang type interpolation operator, see [19], which is given by

$$\Pi_k \xi := \sum_{p \in \mathcal{P}_k} \alpha_p^k(\xi) \varphi_p^k, \quad \alpha_p^k(\xi) := \int_{E_p^k} \psi_p^k(x) \xi(x) dx, \tag{3.4}$$

where $E_p^k \in \mathcal{E}_k$ is an edge starting from p, and ψ_p^k is the dual of φ_p^k defined by

$$\int_{E_p^k} \psi_p^k(x) \varphi_q^k(x) = \delta_{pq} \quad \forall q \in \mathcal{P}_k.$$

We note that using standard nodal basis functions φ_p^k, $\varphi_p^k(q) = \delta_{pq}$, and a piecewise linear dual function ψ_p, we can ensure that ψ_p^k is bounded by $\|\psi_p^k\|_{L^\infty(E_p^k)} \lesssim h_k^{-1}$ (c.f. [19, Lemma 3.1]).

The essential point to preserving homogeneous Dirichlet boundary conditions is the correct choice of E_p^k. For $p \in \Gamma_D$, we require $E_p^k \subset \Gamma_D$ which is possible due to assumption (A2). This leads to $\Pi_k \xi \in V_k^-$ for $\xi \in H^1_{0,D}(\Omega)$ and $\|(\mathrm{Id} - \Pi_k)\zeta\|_1 \lesssim h_k^s \|\zeta\|_{1+s}$ for all $\zeta \in H^{1+s}(\Omega)$ (c.f. [19, Theorem 4.1]) and the approximation property for V_k^- follows.

Since we are going to study the approximation property for the spaces V_k^+, we have to estimate the coefficients of the Scott–Zhang operator for the vertices near the change between Dirichlet and Neumann boundary conditions. This estimate is given in the following lemma.

LEMMA 3.1. *Let $0 \le s < 1/2$, $p \in \mathcal{P}_k$ and $R_0 \in \mathcal{E}_k$ with $|p - y| \lesssim h_k \quad \forall y \in R_0$. For $\zeta \in H^{1+s}(\Omega)$ with $\int_{R_0} \zeta(y)dy = 0$, there exists a neighborhood Ω_p of p such that $\operatorname{diam}(\Omega_p) \lesssim h_k$ and*

$$\left(\alpha_p^k(\zeta)\right)^2 \lesssim h_k^{2s} \, |\zeta|^2_{1+s,\Omega_p} \, .$$

Proof. Integrating $\left(\alpha_p^k(\zeta)\right)^2$ over R_0 and applying the Cauchy–Schwarz-inequality, we get

$$\begin{aligned}
\left(\alpha_p^k(\zeta)\right)^2 &= \left(\int_{E_p^k} \psi_p^k(x)\zeta(x)dx \right)^2 \\
&= \left(\frac{1}{|R_0|} \int_{R_0} \int_{E_p^k} (\zeta(x) - \zeta(y))\psi_p^k(x)dxdy \right)^2 \\
&= \left(\frac{1}{|R_0|} \int_{R_0} \int_{E_p^k} \frac{\zeta(x) - \zeta(y)}{|x-y|^{s+1}} \psi_p^k(x) \, |x-y|^{s+1} \, dxdy \right)^2 \\
&\le \frac{1}{|R_0|^2} \int_{R_0} \int_{E_p^k} \frac{(\zeta(x) - \zeta(y))^2}{|x-y|^{2s+2}} dxdy \int_{R_0} \int_{E_p^k} \psi_p^k(x)^2 \, |x-y|^{2s+2} \, dxdy.
\end{aligned}$$

Defining $\Xi := E_p^k \cup R_0$ and $m = s + 1/2$, we obtain

$$\int_{R_0} \int_{E_p^k} \frac{(\zeta(x) - \zeta(y))^2}{|x-y|^{2s+2}} dxdy \le \int_\Xi \int_\Xi \frac{(\zeta(x) - \zeta(y))^2}{|x-y|^{2m+1}} dxdy = |\zeta|^2_{m,\Xi} \, .$$

We note that the set Ξ does not have to be connected. For $x \in E_p^k$ and $y \in R_0$, we have $|x - y| \lesssim h_k$ and using $\left|E_p^k\right| \approx h_k \approx |R_0|$, we obtain $\operatorname{diam}(\Xi) \lesssim h_k$. As $\left\|\psi_p^k\right\|_{L^\infty(E_p^k)} \lesssim h_k^{-1}$, we find the following upper bound for the second integral,

$$\int_{R_0} \int_{E_p^k} \psi_p(x)^2 \, |x-y|^{2s+2} \, dxdy \lesssim |R_0| \, |E_p^k| \, h_k^{-2} h_k^{2s+2} \approx |R_0|^2 \, h_k^{2s} \, ,$$

and thus

$$\left(\alpha_p^k(\zeta)\right)^2 \lesssim \frac{1}{|R_0|^2} \, |R_0|^2 \, h_k^{2s} \, |\zeta|^2_{m,\Xi} \lesssim h_k^{2s} \, |\zeta|^2_{s+1/2,\Xi} \, .$$

With a suitable set Ω_p such that $\Xi \subseteq \partial\Omega_p$, we get the result by applying the trace theorem. ∎

Using Lemma 3.1, it is now easy to establish a suitable approximation property for V_k^+ and V_k^{mod}.

THEOREM 3.2. *The finite element spaces V_k^+, V_k^-, V_k^{mod} satisfy the approximation property for $0 \le s < 1/2$,*

$$\inf_{v \in W_k} \|\zeta - v\|_1 \lesssim h_k^s \, |\zeta|_{1+s} \quad \forall \zeta \in H^{1+s}_{0,D}(\Omega), \quad W_k \in \{V_k^+, V_k^-, V_k^{mod}\}. \tag{3.5}$$

Proof. The approximation property for the space V_k^- follows directly from the definition of Π_k.

We recall that $V_k^+ \subseteq V_k^{\mathrm{mod}}$, and thus we can restrict ourselves to V_k^+. Each function $v \in V_k^-$ can be written in terms of $v = v^+ + \Delta v$ where $v^+ \in V_k^+$, and Δv is a linear combination of finite element basis functions associated with vertices $p \in \Delta\mathcal{P} := \mathcal{P}_k^- \setminus \mathcal{P}_k^+$ near the change in the type of boundary conditions. For a given $\zeta \in H^{1+s}_{0,D}(\Omega)$, we set $v := \Pi_k \zeta$. By the choice of Π_k, v is an element of V_k^-, and the estimate $\|\zeta - v\|_1 \lesssim h_k^s \, |\zeta|_{1+s}$ holds. In order to get the same result for v^+, it remains to derive an upper bound of $\|\Delta v\|_1$.

We write $\Delta v = \sum_{p\in\Delta\mathcal{P}} \alpha_p^k \varphi_p^k$. For each $p \in \Delta\mathcal{P}$, we find a vertex $q \in \Gamma_D$ such that $|p - q| \lesssim h_k$. Using Assumption (A2), we can find an edge $R_0 \in \mathcal{E}_k$ with $R_0 \subset \Gamma_D$. With this choice of R_0 and with $\zeta \in H^{1+s}_{0,D}(\Omega)$, the Assumptions in Lemma 3.1 are obviously satisfied. We use that Ω_p is a local neighborhood of p and get

$$\begin{aligned}\|\Delta v\|_0^2 &\approx h_k^2 \sum_{p\in\Delta\mathcal{P}} \left(\alpha_p^k\right)^2 \lesssim h_k^2 \sum_{p\in\Delta\mathcal{P}} h_k^{2s} \, |\zeta|^2_{s+1,\Omega_p} \\ &= h_k^{2(s+1)} \sum_{p\in\Delta\mathcal{P}} |\zeta|^2_{s+1,\Omega_p} \lesssim h_k^{2(s+1)} \, |\zeta|^2_{1+s} \, .\end{aligned}$$

The inverse estimate applied on Δv yields $\|\Delta v\|_1 \lesssim h_k^{-1} \|\Delta v\|_0$, and thus we obtain

$$\left\|\zeta - v^+\right\|_1 = \|\zeta - v + \Delta v\|_1 \le \|\zeta - v\|_1 + \|\Delta v\|_1 \lesssim h_k^s \, |\zeta|_{1+s} \, .$$

□

REMARK 3.3. *In the 3-dimensional case, the approximation property can be shown using the same arguments.*

REMARK 3.4. *If a higher regularity, $\alpha > 1/2$, is assumed, (3.5) can be shown for $0 \le s \le \alpha$ with similar techniques.*

3.2. Smoothing property. For the spaces V_k^+ and V_k^-, the standard inverse estimate holds, but for the spaces V_k^{mod}, the inverse estimate is not obvious. Because of the hierarchical modification $\tilde{\pi}_k^K$, the elements of V_k^{mod} are no longer finite element functions associated with the triangulation $\mathcal{T}_k$, but only with $\mathcal{T}_K$.

As we have seen, the spaces V_k^{mod} are constructed by using the multiplicative modification operators $\tilde{\pi}_k^K$ on the spaces $\tilde{V}_k^-$, where $\tilde{V}_k^-$ are the non-conforming spaces defined with respect to the enlarged Dirichlet boundary $\tilde{\Gamma}_D$. To show the inverse estimate for these spaces, we proceed as follows. We start by considering the spaces V_k^- and the corresponding modification operators π_k^K and show an inverse estimate for $\pi_k^K V_k^-$ using an additional Assumption (A3) on the boundary conditions. We then show that Assumption (A3) still holds for the enlarged Dirichlet boundary leading to the inverse estimate for V_k^{mod}.

To derive the inverse estimate for $\pi_k^K V_k^-$, we are going to estimate the H^1-norm of a function w, $w = \pi_k^K v$, by the H^1-norm of the unmodified function $v \in V_k^-$. The problem is that the operator $\pi^k : (V_k^-, \|\cdot\|_1) \to H^1(\Omega)$ is bounded, but not by one. Thus the trivial bound for π_k^K would result in an exponential growth. We therefore need to have a more detailed look at the modification as described in Section 2.

We first discuss properties and their consequences for unresolved boundaries. For boundary elements $E \in \mathcal{E}_k$ with a change in the boundary condition, we define the number $0 \le N_k(E) \le 1$ as

$$N_k(E) := \frac{\mathrm{meas}(E \cap \Gamma_N)}{\mathrm{meas}(E)}.$$

This number will be called Neumann-ratio of E. We note that because of Assumption (A1) there is at most one change in the boundary condition on each E. Introducing local coordinates on E such that the corner on Γ_N has local coordinate 0 and the corner on Γ_D has the local coordinate 1, the number $N_k(E)$ describes the local coordinate of the change in the boundary condition. We assume

(A3) There exists a number $0 < S \le 1$ such that $S \le N_k(E)$ or $N_k(E) = 0$ for all $k \ge 0$ and $E \in \mathcal{E}_k$, $E \subset \Gamma$.

Having the modified-basis approach in mind, Assumption (A3) ensures, that the modified basis functions $\pi_k^K \varphi_p^k$ cannot get steeper and steeper with increasing level k.

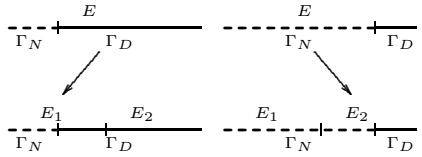

FIGURE 3.1. *Behavior of N_k under refinement*

Let us consider the Neumann-ratio under refinement; see Figure 3.1. The boundary element E on level k with $0 < N_k(E) \leq 1$ is decomposed into E_1 and E_2 on level $k+1$. The indices are chosen such that $E_1 \cap \Gamma_N$ and $E_2 \cap \Gamma_D$ is non-empty. If $N_k(E) \leq \frac{1}{2}$ then $N_{k+1}(E_1) = 2N_k(E)$ and $N_{k+1}(E_2) = 0$. If $N_k(E) > \frac{1}{2}$ then $N_{k+1}(E_1) = 1$ and $N_{k+1}(E_2) = 2N_k(E) - 1$. So, for each $E \in \mathcal{E}_0$ with $0 < N_0(E) < 1$, we define the sequence $(N_k)_k$ by

$$N_0 = N_0(E), \quad N_{k+1} = \begin{cases} 2N_k & N_k \leq \frac{1}{2} \\ 2N_k - 1 & N_k > \frac{1}{2}. \end{cases} \tag{3.6}$$

Note that if the boundary conditions are resolved at some level, the sequence $(N_k)_k$ becomes stationary.

REMARK 3.5. *The sequence $(N_k)_k$ becomes periodic if and only if N_0 is a rational number; this can easily be seen by looking at N_0 in the binary system. If for each $E \in \mathcal{E}_0$ with unresolved boundary conditions, the Neumann-ratio $N_0(E)$ is rational, we can define S as the minimum of all sequences and Assumption (A3) holds trivially.*

We see that because of $V_k^+ \subseteq V_l^+ \subseteq V_l^-$, $0 \leq k \leq l \leq K$, the Lagrange-interpolation π^l is the identity operator for $v \in V_k^+$ and subsequently also for a function $v^- \in V_k^-$ on elements $T \in \mathcal{T}_k$ without a change in the boundary condition. Moreover, we have $\pi^K = \mathrm{Id}$ by definition.

In order to estimate the norm of a modified function in terms of the modified function, we make the estimate element-wise. For interior elements or elements having no change in the boundary condition, the modification operator is the identity and we are finished. Let us consider an element $T \in \mathcal{T}_k$, $0 \leq k < K$, with a boundary element $E \in \mathcal{E}_k \cap \partial\Omega$ having unresolved boundary conditions. The modification here obviously depends only on the Neumann-ratio $N_k(E)$.

By the affine mapping ϖ, the element T is transfered to the reference element $\hat{T}$ which is given by the vertices $\hat{p}_1 = (0,0), \hat{p}_2 = (1,0), \hat{p}_3 = (0,1)$, see Figure 3.2. The operators $\hat{\pi}^k$ and $\hat{\pi}_k^K$ are then defined by $\hat{\pi}^k(x) = \pi|_T(\varpi^{-1}x)$ and $\hat{\pi}_k^K(x) = \pi_k^K|_T(\varpi^{-1}x)$.

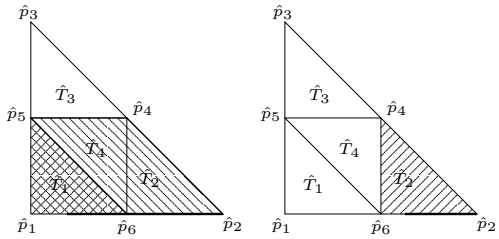

FIGURE 3.2. *Refinement of the reference element $\hat{T}$ into sub-elements $\hat{T}_1, \ldots, \hat{T}_4$. Left: $N_k \leq \frac{1}{2}$, right: $N_k > \frac{1}{2}$. The sub-elements where $\hat{\pi}^{k+1}\hat{v} \neq \hat{v}$ and where $\hat{\pi}^l \neq Id, l > k+1$ are hatched.*

We consider a linear function $\hat{v}$ on $\hat{T}$ with $\hat{v}(\hat{p}_2) = 0$.. Exploiting the fact that $\hat{\pi}^{k+1} = \mathrm{Id}$ on V_k^+, we can distinguish between two cases depending on N_k, see Figure 3.2. If $N_k > \frac{1}{2}$, we see that $\hat{\pi}^{k+1}\hat{v} = \hat{v}$ on $\hat{T}$; if $N_k \leq \frac{1}{2}$, then $\hat{\pi}^{k+1}\hat{v}$ is linear on $\hat{T}_1, \ldots, \hat{T}_4$ with $\hat{\pi}^{k+1}\hat{v}(\hat{p}_6) = 0$. This leads to the following estimate.

LEMMA 3.6. *Let $\hat{T}$ be the reference element (see Figure 3.2) and $\hat{v}$ linear on $\hat{T}$ with $\hat{v}(\hat{p}_2) = 0$. Then for $i = 1, \dots, 4$,*

$$\begin{aligned} \left|\hat{\pi}^{k+1}\hat{v}\right|_{1,\hat{T}_i} &\le |\hat{v}|_{1,\hat{T}}\,, & N_k &\le \frac{1}{2}, \\ \left|\hat{\pi}^{k+1}\hat{v}\right|_{1,\hat{T}_i} &= \frac{1}{4}\,|\hat{v}|_{1,\hat{T}}\,, & N_k &> \frac{1}{2}. \end{aligned}$$

Proof. For $N_k > \frac{1}{2}$, we have $\hat{\pi}^{k+1}\hat{v} = \hat{v}$ and the linearity of $\hat{v}$ gives the proposition. For $N_k \le \frac{1}{2}$, we note that $\hat{\pi}^{k+1}\hat{v}$ is linear on the sub-elements $\hat{T}_1, \dots, \hat{T}_4$ with $\hat{\pi}^{k+1}\hat{v}(\hat{p}_i) = v(\hat{p}_i)$ for $i = 1, \dots, 5$, and $\hat{\pi}^{k+1}\hat{v}(\hat{p}_6) = 0$. A straightforward calculation shows

$$|\hat{v}|^2_{1,\hat{T}} = \frac{1}{2}\left((a-b)^2 + a^2\right), \quad a := v(\hat{p}_1), b := v(\hat{p}_3),$$

$$\begin{aligned} \left|\hat{\pi}^{k+1}\hat{v}\right|^2_{1,\hat{T}_1} &= \frac{1}{2}\left(\left(\frac{a-b}{2}\right)^2 + a^2\right) \le |\hat{v}|^2_{1,\hat{T}}\,, \\ \left|\hat{\pi}^{k+1}\hat{v}\right|^2_{1,\hat{T}_2} &= \frac{1}{2}\left(\frac{b}{2}\right)^2 \le \frac{1}{2}\frac{(a-b)^2 + a^2}{2} \le |\hat{v}|^2_{1,\hat{T}}\,, \\ \left|\hat{\pi}^{k+1}\hat{v}\right|^2_{1,\hat{T}_3} &= \frac{1}{2}\left(\left(\frac{a-b}{2}\right)^2 + \left(\frac{a}{2}\right)^2\right) \le |\hat{v}|^2_{1,\hat{T}}\,, \\ \left|\hat{\pi}^{k+1}\hat{v}\right|^2_{1,\hat{T}_4} &= \frac{1}{2}\left(\left(\frac{a}{2}\right)^2 + \left(\frac{b}{2}\right)^2\right) \le \frac{1}{2}\left(\frac{2(a-b)^2 + 3a^2}{4}\right) \le |\hat{v}|^2_{1,\hat{T}}\,. \end{aligned}$$

□

Now, using that $\hat{\pi}^k$ is the identity on elements without a change in the boundary condition, we see that for $N_k > \frac{1}{2}$, we have $\hat{w} = \hat{\pi}^{k+1}\hat{v} = \hat{v}$ on $\hat{T}_1, \hat{T}_3, \hat{T}_4$ and $\hat{w} = \hat{\pi}^K_{k+1}\hat{\pi}^{k+1}\hat{v} = \hat{\pi}^K_{k+1}\hat{v}$ on $\hat{T}_2$. For $N_k \le \frac{1}{2}$, we obtain $\hat{w} = \hat{\pi}^{k+1}\hat{v} = \hat{v}$ on $\hat{T}_3$ and $\hat{w} = \hat{\pi}^{k+1}\hat{v}$ on $\hat{T}_4$ and $\hat{T}_2$. Furthermore, $\hat{w} = \hat{\pi}^K_{k+1}\hat{\pi}^{k+1}\hat{v}$ on $\hat{T}_1$.

Since $\hat{\pi}^{k+2}$ depends on the Neumann-ratio N_{k+1}, the idea is to find a function depending on N_k such that $|\hat{w}|_1$ can be estimated in terms of $|\hat{v}|_1$.

LEMMA 3.7. *Assume that there exists a function $C : [0,1] \to [1,\infty)$ satisfying*

$$3 + C(2N) \le C(N), \quad S < N \le \frac{1}{2}, \tag{3.7}$$

$$\frac{3 + C(2N-1)}{4} \le C(N), \quad N > \frac{1}{2}. \tag{3.8}$$

Let $0 \le k \le K$, let $\hat{T}$ be the reference element with Neumann-ratio N_k, let $\hat{v}$ be linear on $\hat{T}$ and let $\hat{w} := \hat{\pi}^K_k\hat{v}$. Then the following estimate holds,

$$|\hat{w}|^2_{1,\hat{T}} \le C(N_k)\,|\hat{v}|^2_{1,\hat{T}}\,.$$

Proof. The proof is by induction. Because of $\hat{w} = \hat{v}$ for $k = K$ and $N_k = 0$, these cases are trivial. Considering $k < K$, we have two cases depending on the Neumann-ratio N_k. For $N_k > 1/2$, we have $\hat{w} = \hat{\pi}^K_{k+1}\hat{\pi}^{k+1}\hat{v}$ on $\hat{T}_2$ and $\hat{w} = \hat{\pi}^{k+1}\hat{v}$ on the other sub-elements. As $N_{k+1} = 2N_k - 1$ and $\hat{\pi}^{k+1}\hat{v}$ is linear on $\hat{T}_2$, we obtain using the induction hypothesis

$$|\hat{w}|^2_{1,\hat{T}_2} \le C(N_{k+1})\left|\hat{\pi}^{k+1}\hat{v}\right|^2_{1,\hat{T}_2} = C(2N_k - 1)\left|\hat{\pi}^{k+1}\hat{v}\right|^2_{1,\hat{T}_2}\,.$$

Summing up and applying Lemma 3.6 and (3.8), we get

$$|\hat{w}|^2_{1,\hat{T}} \leq \frac{3 + C(2N_k - 1)}{4} |\hat{v}|^2_{1,\hat{T}} \leq C(N_k) |\hat{v}|^2_{1,\hat{T}} .$$

For $S < N_k \leq 1/2$, we get $\hat{w} = \hat{\pi}^K_{k+1} \hat{\pi}^{k+1} \hat{v}$ on $\hat{T}_1$ and $\hat{w} = \hat{\pi}^{k+1} \hat{v}$ on the other sub-elements. As $N_{k+1} = 2N_k$, we obtain using the induction hypothesis

$$|\hat{w}|^2_{1,\hat{T}_1} \leq C(N_{k+1}) \left|\hat{\pi}^{k+1} \hat{v}\right|^2_{1,\hat{T}_1} \leq C(2N_k) \left|\hat{\pi}^{k+1} \hat{v}\right|^2_{1,\hat{T}_1} .$$

Summing up and applying Lemma 3.6 and (3.7) yield

$$|\hat{w}|^2_{1,\hat{T}} \leq (3 + C(2N_k)) |\hat{v}|^2_{1,\hat{T}} \leq C(N_k) |\hat{v}|^2_{1,\hat{T}} .$$

□

According to Lemma 3.7, it is now sufficient to define a bounded function $C(\cdot)$ satisfying (3.7) and (3.8) to estimate the H^1-seminorm of a modified function $\hat{w} = \hat{\pi}^K_k \hat{v}$ on the reference element.

LEMMA 3.8. *Assume that (A3) holds and let $0 \leq k \leq K$, let $\hat{T}$ be the reference element with Neumann-ratio N_k, let $\hat{v}$ be linear on $\hat{T}$ and let $\hat{w} := \hat{\pi}^K_k \hat{v}$. Then there exists $0 < C < \infty$ such that*

$$|\hat{w}|^2_{1,\hat{T}} \leq C \ln(\frac{1}{S}) |\hat{v}|^2_{1,\hat{T}} .$$

Proof. By Assumption (A3), $N_k \geq S$; then there exists $M \in \mathbb{N}, M > 1$ such that $S2^M \leq S$. We define $C_M : [0,1] \to \mathbb{R}$ by

$$C_M(N) := \begin{cases} 1 & N \leq \frac{1}{2^M}, \\ 1 + M + 3m & N \in (\frac{1}{2^{m+1}}, \frac{1}{2^m}], 0 \leq m \leq M - 1. \end{cases}$$

We note that the upper bound of $C_M(\cdot)$ is independent of N. A straightforward calculation shows that for $N \in [0,1]$, $C_M(N)$ is bounded by $1 \leq C_M(N) \leq 4M - 2 \leq C \ln(\frac{1}{S})$. Moreover, the Assumptions (3.7) and (3.8) are satisfied. □

To obtain a bound for the condition number, we have to estimate the L^2-norm of a modified function.

LEMMA 3.9. *Let $\hat{T}$ be the reference element, let $\hat{v}$ be linear on $\hat{T}$ and let $\hat{w} = \hat{\pi}^K_k \hat{v}$. Then, the following estimate holds:*

$$\|\hat{w}\|_{0,\hat{T}} \approx \|\hat{v}\|_{0,\hat{T}} .$$

Proof. It can be easily seen that $\hat{v}|_{\hat{T}_3} = \hat{w}|_{\hat{T}_3}$. As $\hat{v}$ is linear on $\hat{T}$, we get

$$\|\hat{v}\|^2_{0,\hat{T}} \lesssim \|\hat{v}\|^2_{0,\hat{T}_3} = \|\hat{w}\|^2_{0,\hat{T}_3} \leq \|\hat{w}\|^2_{0,\hat{T}} .$$

On the other hand, we see that $|\hat{w}(x)| \leq |\hat{v}(x)|$ for all $x \in \hat{T}$, and therefore $\|\hat{w}\|_{0,\hat{T}} \leq \|\hat{v}\|_{0,\hat{T}}$. □

Using Lemma 3.8 and 3.9, we can deduce the inverse estimate for the space $\pi^K_k V^-_k$.

THEOREM 3.10. *For $v \in V^-_k$, the following estimate holds,*

$$\left\|\pi^K_k v\right\|_1 \lesssim h_k^{-1} \left\|\pi^K_k v\right\|_0 .$$

Proof. We set $w := \pi^K_k v$ and note that for v, the standard inverse estimate holds. Applying the transformation rule and summing over all elements $T \in \mathcal{T}_k$, Lemma 3.8 and Lemma 3.9 turn into

$$|w|_1 \lesssim |v|_1 , \quad \|w\|_0 \approx \|v\|_0 .$$

Combining the results, we obtain

$$\|w\|_1^2 = \|w\|_0^2 + |w|_1^2 \lesssim \|v\|_0^2 + |v|_1^2 = \|v\|_1^2 \lesssim h_k^{-2} \|v\|_0^2 \approx h_k^{-2} \|w\|_0^2 .$$

□ We have seen, that under Assumption (A3) the modification π_k^K still preserves the inverse estimate for the modified finite element space. Thus, the inverse estimate also holds for the spaces V_k^{mod} under corresponding conditions. We show now, that Assumption (A3) still holds for the enlarged Dirichlet boundary and hence (A3) is a sufficient condition for the inverse estimate for V_k^{mod}.

LEMMA 3.11. *Let the triangulation $\mathcal{T}$ and Γ_D fulfill Assumption (A3). Then (A3) also holds for $\mathcal{T}$, $\tilde{\Gamma}_D$.*

Proof. By construction of $\tilde{\Gamma}_D$, we have

$$\tilde{N}_k(E) = \frac{[2^K N_k(E)]}{2^K},$$

where $[a] = \max\{n \in \mathbb{N} : n \leq a\}$. With

$$\tilde{K} := \min\{K \in \mathbb{N} : [2^K S] > 0\},$$

we show in the following that using $\tilde{S} := (\frac{1}{2})^{\tilde{K}}$ the triangulation $\mathcal{T}$ with Dirichlet boundary $\tilde{\Gamma}_D$ fulfill Assumption (A3).

First of all, we see that $N_k(E) = 0$ implies $\tilde{N}_k(E) > 0$. Assuming that $\tilde{N}_k(E) > 0$, we use (A3) and obtain $N_k(E) \geq S$ and thus $\frac{[2^K N_k(E)]}{2^K} \geq \frac{[2^K S]}{2^K} \geq (\frac{1}{2})^K$.

Therefore, for $K \leq \tilde{K}$, the given bound holds. For $K > \tilde{K}$, we conclude

$$\frac{[2^K S]}{2^K} \geq \frac{2^{K-\tilde{K}}[2^{\tilde{K}} S]}{2^K} \geq \frac{2^{K-\tilde{K}}}{2^K} = \frac{1}{2^{\tilde{K}}}$$

□

THEOREM 3.12 (Inverse estimate for the space V_k^{mod}). *Let $\tilde{w} \in V_k^{mod}$. Then the inverse estimate holds, i.e.,*

$$\|\tilde{w}\|_1 \lesssim h_k^{-1} \|\tilde{w}\|_0 .$$

Proof. Using Lemma 3.11, we see that Assumption (A3) holds for the enlarged Dirichlet boundary, $\tilde{\Gamma}_D$. Applying Theorem 3.10 gives the proposition. □

4. Numerical examples. In this section, we apply our approaches to the Laplace and the Lamé equation. The numerical examples illustrate the theoretical results. We examine the convergence rates for different problem settings and compare the efficiency of the multigrid algorithm for the three approaches. In our last example, we apply our methods to contact problems. In that case, the change between Dirichlet and and Neumann boundary conditions depends on the solution, and we cannot expect that the coarse meshes will reflect this correctly. The multigrid algorithms were implemented using the software package UG, see [2].

4.1. Laplace equation. We use our methods to solve the Laplace equation, $\Delta u = 0$ on the unit square, $\Omega = (0,1)^2$. On the top of Ω, we impose homogeneous Dirichlet boundary conditions, $u|_{\Gamma_{D,1}} = 0$, and on the bottom we have a unresolved boundary section where we use $u|_{\Gamma_{D,2}} = 1$. The Dirichlet boundary $\Gamma_{D,2}$ in this example is given by $x_0 = 0.2$. For the rest of $\partial\Omega$, we use homogeneous Neumann boundary condition. The problem setting and the numerical solution can be seen in Figure 4.1. We use a Gauß–Seidel iteration as a smoothing operator and one pre- and one post-smoothing step.

First, we examine the relation between the level k and the convergence rates of the multigrid algorithms. The convergence rate is numerically measured by the asymptotic reduction factor of the defect per multigrid cycle.

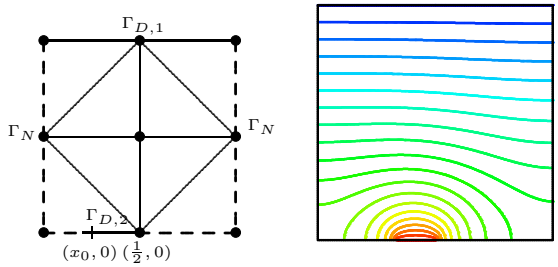

FIGURE 4.1. *Partitioning of the boundary in Γ_D and Γ_N and numerical solution for the Laplace equation*

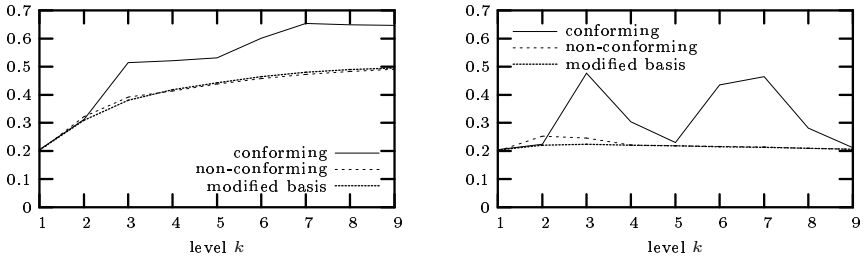

FIGURE 4.2. *Convergence rates for the Laplace equation, left: V-cycle, right: W-cycle*

In Figure 4.2, the convergence rates for the three approaches are shown for the V- and W-cycle algorithm. In the left picture of Figure 4.2, the convergence rates for the V-cycle algorithm are shown. The convergence rates seem to be bounded asymptotically for all our approaches. However, there are large quantitative differences. The conforming approach yields considerably much worse results than the others. The W-cycle algorithm shows convergence rates which are bounded away from one independently of the number of levels. We observe that the non-conforming and the modified-basis approach lead from the beginning to almost constant convergence rates, whereas the conforming approach shows convergence rates which are bounded but oscillate depending on the level. To show that this oscillation comes from the unresolved elements, the convergence rate is compared with the Neumann ratio N_k of the boundary element being not resolved at the level k, see Table 4.1. We see that for some critical values, e.g. 0.6 and 0.2, we find bad convergence rates, whereas a Neumann-ratio of 0.8 always results in qualitative better convergence rates. Hence, there is obviously a correlation between the bad convergence rates of the conforming approach and the unresolved boundary.

level k	3	4	5	6	7	8	9
Neumann-ratio N_k	0.2	0.4	0.8	0.6	0.2	0.4	0.8
convergence rate	0.48	0.3	0.23	0.43	0.46	0.28	0.21

TABLE 4.1
Relation between convergence rates and Neumann-ratio (conforming approach)

For the modified-basis approach, we see that the modification resulting in conforming finite element spaces does not change the stable behavior of the convergence rates. Thus, the modified-basis approach turns out to be both conforming and stable. This holds for both the V- and the W-cycle algorithm.

We now consider the relation between the number of pre- and post-smoothing steps and the convergence rates. We compare the convergence rate on level $k = 6$ for different numbers of smoothing steps. From the results in [11], we expect that the convergence rates for the V-cycle

algorithm will satisfy

$$\kappa \simeq \frac{C}{C + (m_1 m_2)^{\alpha/2}},$$

where κ is the numerical convergence rate, C is a positive mesh- and level-independent constant and m_1, m_2 are the number of pre- and postsmoothing steps. We recall that α is the regularity parameter of the solution. We use $m_1 = m_2 = m$ and thus expect

$$\frac{1}{\kappa} - 1 \simeq C^{-1} m^{\alpha}.$$

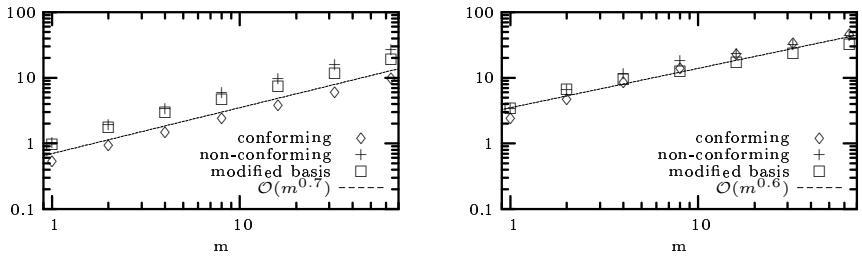

FIGURE 4.3. *Connection between* $\frac{1}{\kappa} - 1$ *and the number of smoothing steps* m*, left: V-cycle, right: W-cycle*

The results for $m = 2^i$, $i = 0, \ldots, 6$ are shown in Figure 4.3. We observe for the V-cycle and for the W-cycle a behavior of $\frac{1}{\kappa} - 1 \approx m^{0.7}$ and $\frac{1}{\kappa} - 1 \approx m^{0.6}$, respectively. From the theoretical point of view, we can only expect m^{α} with the regularity parameter $\alpha < 1/2$.

4.2. Linear elasticity. In our second example, we consider a linear elasticity problem,

$$-\operatorname{div} \sigma(u) = f,$$

where the stress tensor σ is given by Hooke's law using the symmetric and positive definite tensor C,

$$\sigma_{ij} := C_{ijml}\varepsilon_{ml}, \quad C_{ijml} := \frac{E\nu}{(1+\nu)(1-2\nu)}\delta_{ij}\delta_{ml} + \frac{E}{2(1+\nu)}(\delta_{im}\delta_{jl} + \delta_{il}\delta_{jm}).$$

In our example, ε denotes the linearized strain tensor,

$$\varepsilon(u) := \frac{1}{2}\left(\nabla u + (\nabla u)^{\mathsf{T}}\right),$$

and the material parameters are given by $E = 200$ and $\nu = 0.3$.

We model a beam, $\Omega = (0, 10) \times (0, 1)$, that is clamped on the left and piecewise supported on the lower part. On the left, we have homogeneous Dirichlet boundary conditions in the normal and tangential directions, i.e., $u = (0, 0)^{\mathsf{T}}$. On the upper side, we use the Neumann data $n_{\Gamma}^{\mathsf{T}}\sigma(u) = (0, -0.001x)^{\mathsf{T}}$. On the lower side, we have a unresolved segment $(0, 2.4)$, where we impose homogeneous Dirichlet data. On the other segment, $(2.4, 10)$, we impose homogeneous Neumann data.

Because we are interested in application of our method to contact problems, we also consider a second setting. Now, Dirichlet boundary conditions on the lower part are only assumed in normal direction, whereas homogeneous Neumann boundary conditions are applied in tangential direction. The two problem settings can be seen in the upper part of Figure 4.4. The pictures in the middle show the deformed bodies with the effective von Mises stress. The convergence rates for the W-cycle with a Gauß–Seidel smoother and two pre- and postsmoothing steps are shown in the lower diagrams.

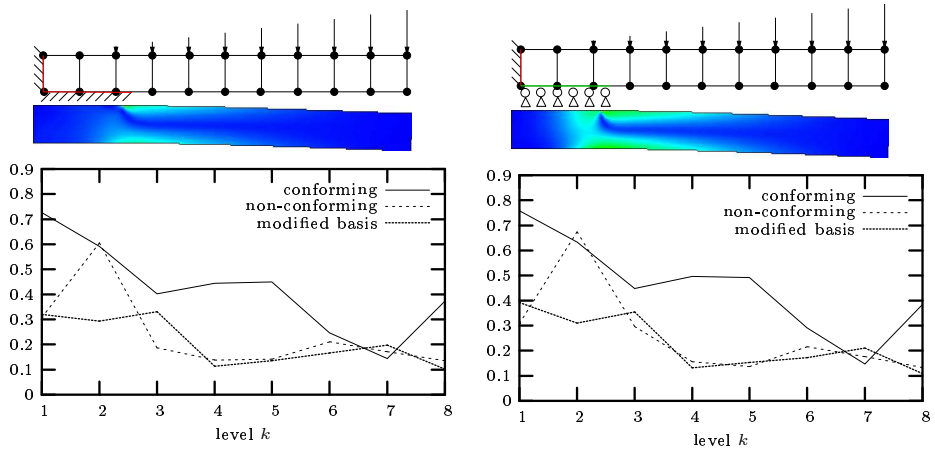

FIGURE 4.4. *Convergence rates for the linear elasticity problem. Left: Dirichlet boundary condition in normal and tangential direction. Right: Different boundary conditions used for normal and tangential direction*

We find that the numerical convergence rates are almost identical in the two settings. This is in good agreement with our observation that the convergence rate depends strongly on the Neumann-ratio; it is the same for both settings. Comparing the convergence rates of the non-conforming and modified-basis approach, we see small oscillations in both cases, whereas for the conforming approach we find the same large oscillations depending in the Neumann ratio as in the case of the Laplace problem.

4.3. Application to contact problems. We consider the two-body contact problem depicted in Figure 4.5, see also [15]. The lower body is given by $\Omega_m := (0, 0.01) \times (0, 0.01)$ and the upper body by $\Omega_s := (0, 0.01) \times (0.01, 0.02)$. As material parameters, we use $E = 15 \times 10^9$ and $\nu = 0.2$ on Ω_m and $E = 20 \times 10^9$ and $\nu = 0.4$ on Ω_s. At the lower boundary of Ω_m and at the upper boundary of Ω_s, we use homogeneous Dirichlet data. On the right side of Ω_m, we impose Neumann boundary conditions, $n_\Gamma^\intercal \sigma(u) = (10^5, -10^6)^\intercal$, and on the left side of Ω_s, $n_\Gamma^\intercal \sigma(u) = (-10^5, -10^6)^\intercal$. For the left side of Ω_m and the right side of Ω_s, we use homogeneous Neumann boundary condition and on the possible contact zone Γ_C the Signorini contact conditions, see, e.g., [16]. To find the correct contact set, we use a primal-dual active set strategy, see [15]. We note that on the correct contact set, Dirichlet boundary conditions are given in normal direction and Neumann boundary condition elsewhere. The type of boundary condition is then resolved on the actual level, but not necessarily on the coarser levels.

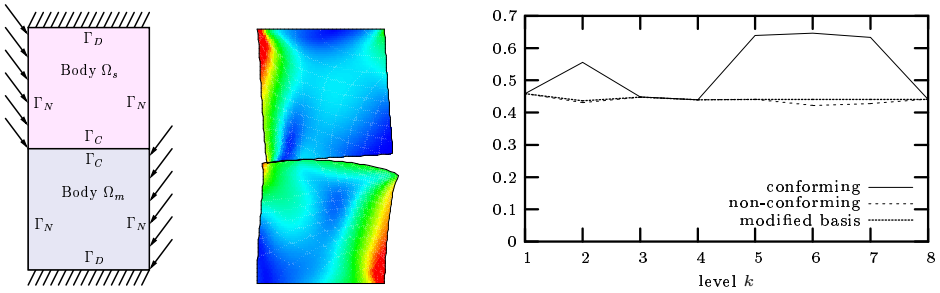

FIGURE 4.5. *Two-body contact problem. Problem definition (left), deformed bodies with effective stress (middle) and convergence rates of the linear problem (right).*

The problem was solved using our three approaches for all active set iterations. We present the results for the multigrid iterations for the linear contact problem, i.e. for the problem where the correct active set is already found. The convergence rates of the W-cycle algorithm using a

symmetric Gauß–Seidel smoother and two pre- and postsmoothing steps are given in Figure 4.5. We encounter the same qualitative results as in the other examples. The convergence rates for all approaches are bounded independently of the number of levels, but the conforming approach shows oscillations whereas for the non-conforming and modified-basis approaches the convergence rates are stable.

REFERENCES

[1] R. E. Bank and T. F. Dupont. An optimal order process for solving finite element equations. *Math. Comp.*, 36:35–51, 1981.

[2] P. Bastian, K. Birken, K. Johannsen, S. Lang, N. Neuß, H. Rentz-Reichert, and C. Wieners. UG - a flexible software toolbox for solving partial differential equations. *Comput. Vis. Sci.*, pages 27–40, 1997.

[3] D. Braess. *Finite Elements. Theory, Fast Solvers and Applications in Solid Mechanics.* Cambridge University Press, 2001.

[4] D. Braess, W. Dahmen, and C. Wieners. A multigrid algorithm for the mortar finite element method. *SIAM J. Numer. Anal.*, 37:48–69, 1999.

[5] D. Braess, M. Dryja, and W. Hackbusch. A multigrid method for nonconforming fe-discretisations with application to non-matching grids. *Computing*, 63:1–25, 1999.

[6] D. Braess and W. Hackbusch. A new convergence proof for the multigrid method including the V-cycle. *SIAM J. Numer. Anal.*, 20:967–976, 1983.

[7] D. Braess and R. Verfürth. Multigrid methods for nonconforming finite element methods. *SIAM J. Numer. Anal.*, 27:979–986, 1990.

[8] J. H. Bramble. *Multigrid methods.* Pitman, New York, 1993.

[9] J. H. Bramble, J. E. Pasciak, J. Wang, and J. Xu. Convergence estimates for multigrid algorithms without regularity assumptions. *Math. Comp.*, 57:23–45, 1991.

[10] S. C. Brenner. Convergence of nonconforming multigrid methods without full elliptic regularity. *Math. Comp.*, 68:25–53, 1999.

[11] S. C. Brenner. Convergence of the multigrid V-cycle algorithm for second-order boundary value problems without full elliptic regularity. *Math. Comp.*, 71:507–525, 2001.

[12] S. C. Brenner and L. R. Scott. *The mathematical theory of finite element methods.* Springer-Verlag, New York/Berlin/Heidelberg, 2002.

[13] P. Grisvard. *Elliptic problems in nonsmooth domains.* Pitman, Boston/London/Melbourne, 1985.

[14] W. Hackbusch. *Multi-Grid methods and Applications.* Springer, Berlin, Heidelberg, 1985.

[15] S. Hüeber and B. Wohlmuth. A primal-dual active set strategy for non–linear multibody contact problems. *Comput. Methods Appl. Mech. Engrg*, 194:3147–3166, 2005.

[16] N. Kikuchi and J. Oden. *Contact problems in elasticity: A study of variational inequalities and finite element methods.* SIAM Studies in Applied Mathematics 8, Philadelphia, 1988.

[17] R. Kornhuber and R. Krause. Adaptive multigrid methods for Signoriniś problem in linear elasticity. *Comput. Vis. Sci.*, 4:9–20, 2001.

[18] N. Neuss and C. Wieners. Criteria for the approximation property for multigrid methods in nonnested spaces. *Math. Comp.*, 73:1583–1600 (electronic), 2004.

[19] L. R. Scott and S. Zhang. Finite element element interpolation of nonsmooth functions satisfying boundary conditions. *Math. Comp.*, 54:483–493, 1990.

[20] A. Weiß. *Mehrgittermethoden zu elliptischen Randwertproblemen bei nicht aufgelöstem Dirichlet/Neumann-Übergang.* Diploma thesis, Universität Stuttgart, 2004.

[21] B. I. Wohlmuth and R. Krause. Monotone methods on non-matching grids for non linear contact problems. *SIAM J. Sci. Comput.*, 25:324–347, 2002.

Erschienene Preprints ab Nummer 2005/001

Komplette Liste: `http://preprints.ians.uni-stuttgart.de`

2005/001 *Nicaise, S., Sändig, A.-M.:* Dynamical crack propagation in a 2D elastic body. The out-of plane state.

2005/002 *Hüeber, S., Matei, A., Wohlmuth, B.I.:* A mixed variational formulation and an optimal a priori error estimate for a frictional contact problem in elasto-piezoelectricity

2005/003 *Sändig, A.-M.:* Distributionentheorie mit Anwendungen auf partielle Differentialgleichungen. Vorlesung im Wintersemester 2004/2005

2005/004 *Sändig, A.-M., Buchukuri, T., Chkadua, O., Natroshvili, D.:* Solvability and regularity results to boundary-transmission problems for metallic and piezoelectric elastic materials

2005/005 *Flemisch, B., Wohlmuth, B.I.:* Stable Lagrange multipliers for quadrilateral meshes of curved interfaces in 3D

2005/006 *Geis, W.:* Determination of stress singularities in piezoelectric stack actuators

2005/007 *Geis, W.:* Numerical simulation of linear models for piezoelectric stack actuators

2005/008 *Sändig, A.-M.:* Mathematische Methoden in der Kontinuumsmechanik. Vorlesung im Sommersemester 2005

2005/009 *Lehrstuhl N.N. (Wendland), Lehrstuhl Wohlmuth, Abteilung Sändig, Abteilung Gekeler:* Jahresbericht 2005

2005/010 *Brunßen, S., Schmid, F., Schäfer, M., Wohlmuth, B.:* A fast and robust method for contact problems by combining a primal-dual active set strategy and algebraic multigrid methods

2005/011 *Weiss, A., Wohlmuth, B.:* Multigrid methods for unresolved Dirichlet boundaries